Attempted Oxidative Generation of a Dihydrogen Complex

Andrei A. Zlota,[1a] Mats Tilset,*[,1b] and Kenneth G. Caulton*[,1a]

Departments of Chemistry, Indiana University, Bloomington, Indiana 47405, and University of Oslo, P.O. Box 1033, Blindern, N-0315 Oslo, Norway

Received March 23, 1993

Cyclic voltammetry of **1**, $Cp^*Ru(P)(H)_3$ (P = PPh_3), in MeCN at a gold electrode (20 °C, 1 V/s) is irreversible but produces in high yield **2**, $Cp^*RuP(MeCN)_2^+$, which does show a reversible cyclic voltammogram. The reaction consumes 1 faraday/mol of Ru, and thus all hydride ligands are converted to H_2. Sweep rate and low-temperature studies, chemical trapping, and chemical oxidation (with Cp_2Fe^+) are consistent with $\mathbf{1}^{\bullet+}$ reacting by proton transfer to **1**, to form transient **3**, $Cp^*RuPH_4^+$. This species was independently synthesized by protonation of **1** at low temperature in CH_2Cl_2 and was characterized by NMR spectroscopy. It reacts rapidly with MeCN to produce first $Cp^*RuPH_2(MeCN)^+$ and H_2 and then **2**. Proton T_1 relaxation time measurements suggest **3** contains at least one H_2 molecule. Cyclic voltammetry at a Pt electrode shows curve crossings whose origin is traced to adsorption and then oxidation of H_2 released from the metal complex(es).

Introduction

The one-electron oxidation of neutral 18-electron organotransition-metal hydrides generates cation radicals whose Brønsted acidities are greatly enhanced (by *ca.* 20 pK_a units)[2] when compared to the acidities of their neutral parent complexes.[2,3] These cation radicals therefore are prone to undergo deprotonation, a reaction which represents a formal two-electron reductive dissociation from the cation radical (eq 1). This behavior has been noted for several monohydrides[2] and also for several polyhydrides.[3]

$$M\text{–}H \rightarrow M\text{–}H^{\bullet+} \rightarrow M^{\bullet} + H^+ \qquad (1)$$

The cation radicals of species containing two or more hydride ligands may in principle undergo a formal intramolecular two-electron transfer by a coupling of the hydrides to generate a coordinated dihydrogen ligand (eq 2).[4] Such a process is likely

$$L_nM(H)_2 \rightarrow L_nM(H_2)^{\bullet+} \rightarrow L_nM(H_2)^{\bullet+} \rightarrow L_nM(H)^{\bullet} + H^+ \qquad (2)$$

to be triggered by one-electron oxidation if the metal is already in a high oxidation state. Considering that dihydrogen complexes have been found to be somewhat *more* acidic (on the order of 1 pK_a unit) than isomeric dihydrides,[5a] proton transfer may well succeed the hydride-coupling reaction.

Following the original discovery of dihydrogen complexes,[6] the question of whether compounds previously considered to be polyhydrides should be reformulated as species containing one or more dihydrogen ligands arose.[4] Among the methods that have been devised to resolve the case, one of the most well-known is the measurement of the T_1 relaxation times of the hydrides by ^1H NMR, as well as $^1J_{HD}$ coupling constants of partially deuterated species.[4a]

Later, it was suggested that electrochemical methods may be used to differentiate between classical (hydride) and nonclassical (dihydrogen) structures for relatively high-oxidation-state polyhydrides.[3b,7] The electrode potential for the oxidation of a nonclassical structure should be considerably lower than that of the isomeric classical structure because the classical structure has a formal oxidation state two steps higher than the nonclassical.

In this paper, we present the details of an investigation of the oxidation chemistry of the *classical*, high-oxidation-state ruthenium hydride $Cp^*Ru(PPh_3)(H)_3$ (**1**; $Cp^* = \eta^5\text{-}C_5Me_5$). Compound **1** undergoes a one-electron oxidation to yield a transient cation radical, which may represent a dihydrogen species. A cascade of reactions rapidly takes place, starting with deprotonation and subsequent liberation of molecular hydrogen. This evolved molecular hydrogen has a profound effect on the voltammetric behavior of **1**, and this issue will be specifically addressed.

Results and Discussion

Electrochemical Oxidation of $Cp^*Ru(PPh_3)(H)_3$ (1) at the Au Electrode. The oxidative behavior of **1** in acetonitrile was investigated by cyclic voltammetry (CV). Figure 1 shows a cyclic voltammogram for the oxidation of **1** at an Au disk electrode (d = 0.4 mm) in acetonitrile/0.1 M $Bu_4N^+PF_6^-$ (20 °C, voltage sweep rate v = 1.0 V/s). The voltammogram shows a chemically irreversible wave for the oxidation of **1** at peak a (peak potential E_p = 0.13 V vs the ferrocene/ferrocenium (Fc) couple; separation peak and half-peak potentials $E_p - E_{p/2}$ = 0.120 V). A chemically nearly reversible couple due to the oxidation of a product arising from follow-up reactions of $\mathbf{1}^{\bullet+}$ is located at peak b (reversible oxidation potential taken as the midpoint between the anodic and cathodic peaks, E_{rev} = 0.42 V vs Fc; anodic to cathodic peak

(1) (a) Indiana University. (b) University of Oslo.
(2) (a) Ryan, O. B.; Tilset, M.; Parker, V. D. *J. Am. Chem. Soc.* **1990**, *112*, 2618. (b) Ryan, O. B.; Tilset, M.; Parker, V. D. *Organometallics* **1991**, *10*, 298. (c) Ryan, O. B.; Tilset, M. *J. Am. Chem. Soc.* **1991**, *113*, 9554. (d) Ryan, O. B.; Smith, K.-T.; Tilset, M. *J. Organomet. Chem.* **1991**, *421*, 315. (e) Klingler, R. J.; Huffman, J. C.; Kochi, J. K. *J. Am. Chem. Soc.* **1980**, *102*, 208.
(3) (a) Westerberg, D. E.; Rhodes, L. F.; Edwin, J.; Geiger, W. E.; Caulton, K. G. *Inorg. Chem.* **1991**, *30*, 1107. (b) Costello, M. T.; Walton, R. A. *Inorg. Chem.* **1988**, *27*, 2563.
(4) For review of the chemistry of dihydrogen complexes, see: (a) Jessop, P. G.; Morris, R. H. *Coord. Chem. Rev.* **1992**, *121*, 155. (b) Crabtree, R. H. *Acc. Chem. Res.* **1990**, *23*, 95. (c) Kubas, G. J. *Acc. Chem. Res.* **1988**, *21*, 120. (d) Crabtree, R. H.; Hamilton, D. G. *Adv. Organomet. Chem.* **1988**, *28*, 299.
(5) (a) Chinn, M. S.; Heinekey, D. M. *J. Am. Chem. Soc.* **1990**, *112*, 5166. Further study shows that the thermodynamic acidities of the dihydride and dihydrogen tautomers *can*, however, be similar. See: Jia, G.; Morris, R. H. *J. Am. Chem. Soc.* **1991**, *113*, 875. (b) Bautista, M. T.; Cappellani, E. P.; Drovin, S. D.; Morris, R. H.; Schweitzer, C. T.; Sella, A.; Zubkowski, J. D. *J. Am. Chem. Soc.* **1991**, *113*, 4876.
(6) Kubas, G. J.; Ryan, R. R.; Vergamini, P. J.; Wasserman, H. J. *J. Am. Chem. Soc.* **1984**, *106*, 451.
(7) (a) Bianchini, C.; Laschi, F.; Peruzzini, M.; Ottaviani, F. M.; Vacca, A.; Zanello, P. *Inorg. Chem.* **1990**, *29*, 3394. (b) Zanello, P. *Comments Inorg. Chem.* **1991**, *11*, 339.

0020-1669/93/1332-3816$04.00/0 © 1993 American Chemical Society

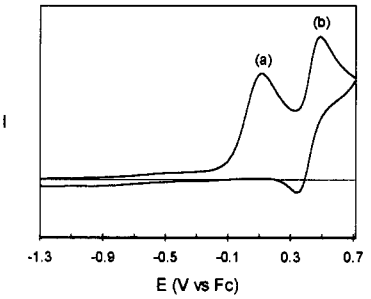

Figure 1. Cyclic voltammogram for the oxidation of **1** (2.0 mM) at an Au disk electrode (d = 0.8 mm) in acetonitrile/0.1 M $Bu_4N^+PF_6^-$ at 20.0 °C and a voltage sweep rate v = 1.0 V/s.

potential separation ΔE_p = 0.140 V). When the solution was seeded with $Cp^*Ru(PPh_3)(NCMe)_2^+BF_4^-$ (**2**(BF_4^-)), the product isolated from the chemical oxidation of **1** in acetonitrile (*vide infra*), wave b gained intensity.

Constant-current coulometry experiments were performed at a Pt mesh working electrode. The disappearance of the substrate was monitored by CV at a separate Au electrode. The experiments indicated the consumption of 1.02 ± 0.03 faradays/mol of charge (average of three separate measurements) for complete disappearance of the substrate oxidation wave at the Au monitoring electrode. When the substrate had been completely consumed, the reversible wave due to **2** was still observed and this product therefore was stable under the reaction conditions. With the voltammogram of an equimolar solution of **2**(BF_4^-) as a reference, the intensity of the product signal indicated that the yield of **2** following the electrolysis of **1** was 86–92%, or nearly quantitative.

The cyclic voltammogram in Figure 1 shows that a significant quantity of **2** is generated on the time scale of the CV experiment. However, it was found that the intensity of oxidation wave b was only ca. 70% of that expected for a quantitative generation of **2**. CV measurements were undertaken at variable sweep rates in the range $0.1 < v < 20$ V/s to see if the instantaneous "yield" of **2** was sweep rate dependent. It was found that the yield converged to 100% at $v < 0.2$ V/s. The apparent yield decreased at higher values of v and was close to 50% at $3 < v < 5$ V/s. At $v > 10$ V/s, significant overlap of peaks a and b precluded reliable yield estimates to be made, but the waveform suggested that the yield did not decrease significantly below 50%. The overall results are in accord with 50% of **2** arising "instantaneously" from $\mathbf{1}^{\bullet+}$ (as seen at high v), followed by another 50% due to a slower process (slow v).

The rather high value for $E_p - E_{p/2}$ for the oxidation of **1** suggests that a non-Nernstian (irreversible) electron transfer takes place. This point will be important in deducing a structure for $\mathbf{1}^{\bullet+}$. This interpretation is supported by the observation that a plot of E_p (measured by derivative cyclic voltammetry (DCV) for improved accuracy)[8] vs log v was linear in the range $0.1 < v < 3$ V/s ($r^2 = 0.996$). The slope $\delta E_p/\delta \log v$ was 0.109 V/decade. For a non-Nernstian process, $\delta E_p/\delta \log v = 1.15RT/\alpha n_a F$, where α is the transfer coefficient and n_a is the number of electrons transferred in the rate-limiting step of the electrode process.[9] Assuming that $n_a = 1$, the data result in $\alpha = 0.27$. In the same range of v, the average value for $E_p - E_{p/2}$ was 0.111 V. For an irreversible electron transfer, this equals $E_p - E_{p/2} = 1.857RT/\alpha n_a F$;[9] our data result in $\alpha = 0.39$ if $n_a = 1$. The discrepancy between the two estimates for α may in part be due to less than ideal behavior of the system. Peak potentials were reproducible to ±10 mV at the Au electrode, whereas the scatter in peak width was considerably greater than this and highly dependent on electrode history (cleaning and polishing). Also, we cannot exclude the possibility that the kinetics for the reaction of $\mathbf{1}^{\bullet+}$ affects the quantitative data at high sweep rates. The scan rate vs V analysis suggests that the value for the standard heterogeneous rate constant k_f° ($=k^\circ \exp[\alpha n_a F(E - E'_0)]$) is small. This can be caused by an intrinsically small value for k° or by a significant kinetic potential shift due to a fast homogeneous follow-up reaction, which will cause the exponential term to be small. A coupling of two hydrides (to generate a dihydrogen ligand) in concert with or immediately after the electron-transfer step would be consistent with either interpretation.

Fast CV experiments failed to outrun the kinetics of the follow-up chemical reaction of $\mathbf{1}^{\bullet+}$. At $v > 10$ V/s, the response was rather poor due to the broad and overlapping waves a and b. The substrate concentration was lowered to 0.25 mM in order to slow down conceivable second-order follow-up reactions (*vide infra*), but this did not provide new information. These experiments indicate that the follow-up reaction has a half-life of less than *ca.* 0.01 s.

Chemical Trapping. When 2 equiv of quinuclidine was added to the electrolyte, wave a in Figure 1 doubled in intensity while the size of peak b only underwent *ca.* 10% increase. Constant-current coulometry measurements were also conducted in the presence of 5 equiv of quinuclidine. In this case, 2.1 ± 0.05 faradays/mol of charge was consumed during the complete oxidation of **1**. The yield of **2**, estimated by measuring the CV peak intensity, again was *ca.* 90%. Workup of the oxidation product mixture revealed that it consisted mostly of **2**(PF_6^-) by comparison of its ^1H NMR spectrum with that of an authentic sample. These results are in accord with a base-induced change from a one-electron to a two-electron oxidation process for **1**, both reactions resulting in the same product **2**. We next sought to identify and synthesize **2** by chemical oxidation.

Chemical Oxidation of $Cp^*Ru(PPh_3)(H)_3$. Oxidation of **1** with the outer-sphere one-electron oxidant $Cp_2Fe^+PF_6^-$ in acetonitrile proceeded according to eq 3 (gas evolution was seen). The reaction

$$Cp^*Ru(PPh_3)(H)_3 \xrightarrow[MeCN]{Cp_2Fe^+PF_6^-} Cp^*Ru(PPh_3)(NCMe)_2^+ + {}^3/_2H_2 + Cp_2Fe \quad (3)$$

was clean and quantitative, as judged by ^1H and $^{31}P\{^1H\}$ NMR spectroscopies, which showed $Cp^*Ru(PPh_3)(NCMe)_2^+$ (**2**) to be the only observable product. The product **2** was independently prepared as its BF_4^- salt by treatment of **1** with $HBF_4 \cdot Et_2O$ in acetonitrile (eq 4) and was characterized by ^1H and $^{31}P\{^1H\}$ NMR

$$Cp^*Ru(PPh_3)(H)_3 \xrightarrow[MeCN]{HBF_4 \cdot Et_2O} Cp^*Ru(PPh_3)(NCMe)_2^+ + 2H_2 \quad (4)$$

spectroscopies. The 1:1 Ru:Fe stoichiometry of eq 3 was established both by reaction with lower amounts of Cp_2Fe^+ (which leaves unreacted $Cp^*Ru(PPh_3)(H)_3$) and by integration (^1H NMR) of the methyl resonances of $Cp^*Ru(PPh_3)(MeCN)_2^+$ against the ring hydrogens of Cp_2Fe.[10] Reaction 3 constitutes an overall one-electron oxidation of **1**, which is in agreement with the coulometry experiments that were conducted in the absence of base.

The oxidation of neutral metal hydrides commonly generates highly Brønsted-acidic cation radicals.[2,3] This was seen to apply to the outer-sphere oxidation of **1** also. When the reaction was performed in the presence of 30 equiv of 2,6-di-*tert*-butyl-4-methylpyridine, 2 equiv of $Cp_2Fe^+PF_6^-$ was needed in order to cause the complete oxidation of **1**. This result is in agreement with the two-electron process that occurred electrochemically

(8) Ahlberg, E.; Parker, V. E. *J. Electroanal. Chem. Interfacial Electrochem.* **1981**, *121*, 73. Parker, V. E. *Electroanal. Chem.* **1986**, *14*, 1.

(9) Bard, A. J.; Faulkner, L. R. *Electrochemical Methods*; Wiley: New York, 1980.

(10) This integration employed long (70 s) FT pulse delays since the protons of Cp_2Fe relax quite slowly.

when the base quinuclidine was added to the electrolyte. The overall stoichiometry of this reaction is shown in eq 5.

$$Cp^*Ru(PPh_3)(H)_3 \xrightarrow[MeCN]{\overset{2Cp_2Fe^+PF_6^-}{\underset{base}{\rightarrow}}} Cp^*Ru(PPh_3)(NCMe)_2^+ + H_2 + H^+ \quad (5)$$

Observation of Intermediates in the Chemical Oxidation of 1. The Brønsted-acidic radical cations of metal hydrides commonly transfer H^+ to their neutral parent hydrides.[2,3] On this basis, the expected primary mode of reaction of $\mathbf{1}^{\bullet+}$ in the absence of other bases is depicted in eq 6.

$$\begin{matrix} Cp^*Ru(PPh_3)H_3^{\bullet+} \\ + \\ Cp^*Ru(PPh_3)(H)_3 \\ \mathbf{1} \end{matrix} \rightarrow \begin{matrix} Cp^*Ru(PPh_3)H_2^{\bullet} \\ + \\ Cp^*Ru(PPh_3)H_4^+ \\ \mathbf{3} \end{matrix} \quad (6)$$

The primary product, $Cp^*Ru(PPh_3)H_2^{\bullet}$, a 17-electron species, could readily be a precursor for the generation of $Cp^*Ru(PPh_3)(NCMe)_2^+$ via a sequence of acetonitrile coordinates, oxidation, and H_2 reductive elimination (no strict order of events intended), whereas the other product, the 18-electron cation $Cp^*Ru(PPh_3)H_4^+$, could readily give rise to the same species by double H_2 elimination and acetonitrile ligation.

The independent synthesis of $Cp^*Ru(PPh_3)H_4^+$ (**3**) was attempted[5] by the low-temperature protonation of **1** with $HBF_4{\cdot}Et_2O$ with the "noncoordinating" solvent dichloromethane-

$$Cp^*Ru(PPh_3)(H)_3 + HBF_4{\cdot}OEt_2 \xrightarrow[-65\ °C]{CD_2Cl_2} \underset{\mathbf{3}}{Cp^*Ru(PPh_3)H_4^+} + BF_4^- + OEt_2 \quad (7)$$

d_2. Indeed, the NMR spectra indicated the clean formation of **3** at −65 °C. The product was quite persistent at −50 °C but rapidly decomposed to several products, including free PPh_3, when the sample was heated to 20 °C. The addition of the acid to an Et_2O solution of **1** at −70 °C generated a precipitate, presumably $\mathbf{3}(BF_4^-)$, but the solid underwent rapid decomposition when the temperature was raised above −60 °C and therefore could not be isolated for further characterization.

The ^1H NMR spectrum of **3** (dichloromethane-d_2, −50 °C) displayed a single hydride signal at δ −7.76 with no observed coupling to phosphorus. The signal had a half-height peak width of 25 Hz (−65 °C, 361 MHz). Lowering the temperature to −90 °C did not lead to development of a more complex pattern resulting from two or more different hydrides.

The intriguing protonation of **1**, already a relatively high formal oxidation state Ru(IV) species, might generate the formally Ru(VI) tetrahydride **3**. This high oxidation state suggests that **3** is a prime candidate for hydride coupling and, if so, should be represented as $Cp^*Ru(PPh_3)(H_2)(H)_2^+$ (Ru(IV)) or $Cp^*Ru(PPh_3)(H_2)_2^+$ (Ru(II)) rather than as $Cp^*Ru(PPh_3)(H)_4^+$. We sought evidence for H–H bonding by protonating $Cp^*Ru(PPh_3)(D)_3$ with $HBF_4{\cdot}Et_2O$ at −76 °C in dichloromethane-d_2. However, the hope of observing a detectable ^1J(H–D) coupling, which would indicate a molecular HD ligand in $Cp^*Ru(PPh_3)HD_3^+$, was not realized. Only a single line (49-Hz width at half-height) was seen at −76 °C.

A short proton T_1 relaxation time can be diagnostic of the presence of an intact H_2 ligand, since T_1 values are reduced by the short distance and hence efficient dipolar relaxation between nuclear spins. In the case at hand, we have a useful standard for comparison of T_1 in the form of the structurally-related conjugate base $Cp^*Ru(PPh_3)(H)_3$. The ^1H NMR $T_{1(min)}$ values for **1** and **3**, respectively (in ms, at 500 MHz, in CD_2Cl_2): 219 (at −42 °C) and 10 (at −52 °C).[11] The data show that the T_1 values for **1** pass through the expected minimum and significantly that this minimum value is about 20 times greater than the minimum value of T_1 for **3**. We propose that this indicates the presence of coordinated H_2 in **3**, but we are unable to distinguish between the formulations $Cp^*Ru^{IV}(PPh_3)(H_2)(H)_2^+$ and $Cp^*Ru^{II}(PPh_3)(H_2)_2^+$.

Each of these formulations readily explains the liberation of H_2 in acetonitrile. Loss of one molecule of H_2 would generate the unsaturated intermediate $Cp^*Ru(PPh_3)H_2^+$. We sought to trap this intermediate by treating **1** with $HBF_4{\cdot}Et_2O$ in dichloromethane-d_2 containing some acetonitrile-d_3. The NMR spectra, obtained at −70 to −65 °C, revealed a new hydride species (singlet by $^{31}P\{^1H\}$ NMR, doublet by ^1H NMR). This species, which we propose is $Cp^*Ru(PPh_3)(NCMe)H_2^+$ (**4**), is transformed to **2** when the temperature is raised (eq 8). The low concentration

$$\underset{\mathbf{3}}{Cp^*Ru(PPh_3)H_4^+} \xrightarrow[-70\ °C]{MeCN} \underset{\mathbf{4}}{Cp^*Ru(PPh_3)(NCMe)H_2^+} \xrightarrow[\Delta]{MeCN} \underset{\mathbf{2}}{Cp^*Ru(PPh_3)(NCMe)_2^+} \quad (8)$$

of **4** relative to **2** and **3** in this experiment (see Experimental Section) suggests that **4**, once formed, is consumed by acetonitrile somewhat faster than **3**.

While **3** is prone to loss of H_2, it also functions as a Brønsted acid. We find that $Cp^*Ru(PPh_3)H_4^+$ reacts smoothly and quantitatively with NEt_3 in dichloromethane-d_2 at −70 °C to yield **1**. While this is entirely consistent with the presence of an intact H_2 ligand in the cationic complex, this finding is not uniquely diagnostic. Complexes with coordinated H_2 are often somewhat more acidic than related dihydride species, but the acidity differences are rather modest[5] and are sometimes reversed (i.e., dihydride more acidic than coordinated H_2).

Discussion of the Nature of $\mathbf{1}^{\bullet+}$ and the Mechanism of Reaction of $\mathbf{1}^{\bullet+}$. So far, we have established that whereas **1** is best represented as a classical Ru(IV) trihydride, the protonation of **1** yields **3**, which, instead of being a Ru(VI) tetrahydride, is a nonclassical Ru(IV) or Ru(II) species containing at least one dihydrogen ligand. What then is the exact nature of $\mathbf{1}^{\bullet+}$, which, if classical, formally is Ru(V)? Due to the rapid (on the CV time scale) reactions of $\mathbf{1}^{\bullet+}$, we have been unable to directly observe $\mathbf{1}^{\bullet+}$ and therefore can only resort to indirect arguments when trying to resolve this question. It was noted during the initial discussion of the CV response of **1** that the half-height peak width was rather large. Such behavior is commonly interpreted to indicate that significant structural/electronic rearrangements occur in concert with the electron transfer.[12] In the case at hand, this would be in accord with a coupling of two hydride ligands being initiated by the oxidation of **1**. Therefore, we suggest that $\mathbf{1}^{\bullet+}$ is indeed at 17-electron, nonclassical dihydrogen complex.

All data presented so far are in accord with the primary reaction of $\mathbf{1}^{\bullet+}$ being as indicated in eq 6, whether $\mathbf{1}^{\bullet+}$ is generated by chemical or electrochemical means. The trapping experiments which led to the detection of **4** suggested that it reacted faster with acetonitrile than does **3**. This observation is consistent with the electrochemical experiments (which were performed under different conditions of concentration and ionic strength): eq 6 suggests the immediate generation of **3** and **4** (the latter from oxidation of $Cp^*Ru(PPh_3)H_2^{\bullet}$, possibly via a 19-electron[13] acetonitrile-coordinated intermediate). If **4** undergoes rapid H_2 elimination, this results in an instantaneous yield of **2** equal to

(11) For $T_{1(min)}$ values for other $Ru(H_2)$ compounds, see: Chung, G.; Arliguie, T.; Chaudret, B. *New J. Chem.* **1992**, *16*, 369.
(12) Geiger, W. E. *Prog. Inorg. Chem.* **1985**, *33*, 275 and references cited.
(13) (a) Trogler, W. C. In *Organometallic Radical Processes*; Trogler, W. C., Ed.; Elsevier: New York, 1990; p 306. (b) Tyler, D. R. *Acc. Chem. Res.* **1991**, *24*, 325.

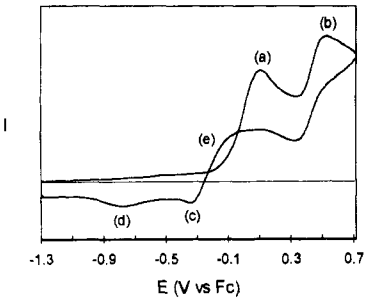

Figure 2. Cyclic voltammogram for the oxidation of **1** (2.0 mM) at a Pt disk electrode (d = 0.6 mm) in acetonitrile/0.1 M $Bu_4N^+PF_6^-$ at 20.0 °C and a voltage sweep rate v = 1.0 V/s.

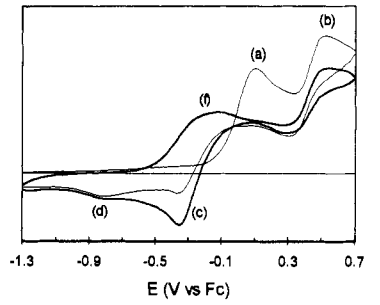

Figure 3. Double-scan cyclic voltammogram for the oxidation of **1** at a Pt disk electrode (d = 0.6 mm). Conditions are given in the caption to Figure 2.

50% in theory—consistent with the CV measurements at v = 3–5 V/s. On a slower time scale, **3** also loses H_2, and as a result, the theoretical yield of **2** on this time scale (v < 0.2 V/s) is 100%.

Electrochemical Oxidation of Cp*Ru(PPh$_3$)(H)$_3$ (1) at the Pt Electrode. Figure 2 shows a cyclic voltammogram for the oxidation of **1** at a Pt disk electrode (d = 0.6 mm) but otherwise under the same experimental conditions as those employed for Figure 1. Again, the voltammogram shows the chemically-irreversible wave for the oxidation of **1** at peak a (peak potential E_p = 0.10 V vs Fc; $E_p - E_{p/2}$ = 0.120 V). The nearly reversible couple due to the oxidation of **2** (verified by seeding the solution with **2**(BF_4^-)) is located at peak b (E_{rev} = 0.44 V vs Fc; ΔE_p = 0.200 V). Two broad waves at –0.34 V (c) and –0.78 V (d) also appear to be due to reaction products. One striking and rather unusual feature in the voltammogram is the crossing of the anodic and cathodic currents near –0.1 V vs Fc (e). This crossing was also observed when the anodic sweep was reversed at 0.30 V vs Fc, and this shows that the curve crossing is not related to the oxidation process at peak b.

As a check for reproducibility, analyses were performed on separately-prepared solutions, and on each solution repeated measurements were performed with and without polishing of the electrode surface between scans. The peak potentials were reproducible to about ±30 mV. The relative intensities of oxidation peaks a and b showed some fluctuations at the Pt electrode. On some occasions, peak d in Figure 2 was nearly absent. However, despite these variations, it was found that the main features of the voltammogram were always qualitatively reproduced.

Double-Scan Cyclic Voltammetry Experiments at the Pt Electrode. Curve-crossing phenomena as seen in Figure 2 are relatively unusual in cyclic voltammetry experiments. Such effects are normally caused by homogeneous redox reactions occurring in the reaction layer next to the electrode surface.[14] The following paragraphs will focus on the source of the curve-crossing phenomena that were observed during the CV measurements at the Pt disk electrode.

Figure 3 shows a double-scan cyclic voltammogram for the oxidation of **1** at the Pt disk electrode. Immediately after the initial scan (fine line), a second scan was initiated (thick line). During the second scan, the original substrate oxidation wave is essentially absent and has been replaced by a new, broad wave f at E_p = –0.11 V vs Fc. This wave appears to be coupled with the wave labeled c in Figure 2. Despite the absence of the substrate wave, the oxidation of the product **2** at 0.44 V still occurs during the second scan. Moreover, the magnitude of the latter wave is more or less unchanged from the first scan. A similar double-scan voltammogram recorded at the Au electrode demonstrated that diffusion of substrate to the electrode surface is efficient enough that significant substrate oxidation occurs on the second scan and that no new signals appear. In contrast, not even a delay time of 60 s (unstirred solution) between two successive scans resulted in complete recovery of the substrate oxidation wave intensity or disappearance of the new oxidation wave f at the Pt electrode. Under these conditions, full signal recovery was seen at the Au electrode.

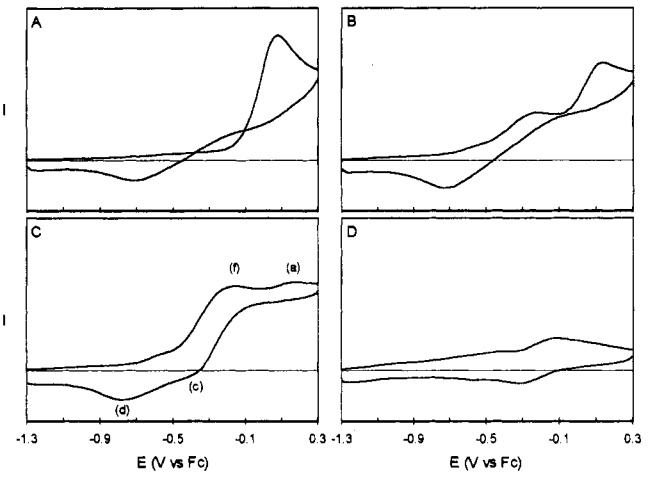

Figure 4. (A–C) Cyclic voltammograms for the oxidation of **1** at a Pt disk electrode (d = 0.6 mm) under an atmosphere of argon (A), 3% H_2/97% N_2 (B), and 10% H_2/90% N_2 (C). (D) Voltammogram of solution saturated with 3% H_2. The voltammograms are drawn on the same scale.

The addition of 2 equiv of quinuclidine caused significant changes in the voltammogram. First, as was seen at the Au electrode, the substrate oxidation wave doubled in intensity whereas the wave for the oxidation of **2** increased by *ca.* 15%. Second, the curve crossing as well as peaks c and d in Figure 2 were absent after the addition of the base.

Electrooxidation of 1 in the Presence of H_2. It occurred to us that one of the obvious products from the oxidation of an already high-oxidation-state metal hydride, namely molecular H_2, could be the source of the peculiar voltammetric behavior at the Pt electrode. The generation of H_2 in the immediate vicinity of the electrode surface could conceivably change the nature of the electrode process. H_2 adsorbs more readily at Pt than at Au, and this could provide an explanation for the significant differences in the electrochemical response at different electrode materials. In order to clarify this point, electrochemical experiments were performed at the Pt and Au electrodes in the presence of H_2. The response at a glassy carbon electrode was also studieid and in all qualitative respects resembled the response of the Au electrode.

Parts A–C of Figure 4 show cyclic voltammograms for the oxidation of **1** at the Pt disk electrode, the scan reversal taking place shortly after the substrate oxidation peak. The voltammogram in Figure 4A was recorded under an argon atmosphere. Figure 4B depicts the same process, but for a solution that was saturated with a 3% H_2/97% N_2 gas mixture. For Figure 4C, a mixture of 10% H_2/90% N_2 was used. In the last two cases, the voltammogram in Figure 4A was fully restored after a 3–4-min vigorous purge with argon. At the Au electrode, the presence

(14) Saveant, J. M. *Acc. Chem. Res.* **1980**, *13*, 323.

of H_2 did *not* alter the appearance of the voltammogram, which only exhibited the chemically-irreversible substrate oxidation wave shown in Figure 1. Figure 4D shows a voltammogram that was recorded for an electrolyte solution saturated with 3% H_2/97% N_2 in the *absence* of **1**. It appears that H_2 undergoes oxidation at the potential where peak f appears in Figure 3. Literature data[15] show that $E°(H^+/H_2)$ in acetonitrile is *ca.* –0.05 V vs Fc. This is in reasonable agreement with our observations here, taking into consideration that our measurements are performed under conditions at which the concentration of H^+ is not under control. It should be emphasized that the trace shown in Figure 4D is the best one ever observed by us for the apparent H_2 oxidation: the appearance of the wave was very sensitive to electrolyte history (cleaning and polishing) and more often was less intense and much broader, and sometimes the wave was hardly discernible.

A CV scan was initiated while the solution containing **1** was vigorously purged with the 3% H_2/97% N_2 mixture. The purging had the effect of increasing the rate of mass transfer to the surface far beyond the capability of the normal diffusional process. This action left the intensity of the first oxidation wave in Figure 4B unchanged, while the second (normal substrate oxidation) wave increased significantly. This observation supports the view that the first wave, not the second, is due to some surface adsorption process.

Attempted Voltammetric Detection of Intermediates 3 and 4. In an attempt to lengthen the lifetime of any intermediates, we have also studied oxidation in a less nucleophilic solvent and at reduced temperature. The oxidation of **1** at the Pt electrode in dichloromethane/0.1 M $Bu_4N^+PF_6^-$ (10 mL) containing one drop of acetonitrile at –40 °C[16] resulted qualitatively in a CV response similar to that of Figure 2. *Ca.* 0.5 μL of $HBF_4·Et_2O$ was added with the hope that **3** could be detected under these conditions. The waves arising from the oxidation of **1** and the product **2** both decreased to *ca.* 20% of the intensity registered in the absence of acid. An irreversible peak was seen at *ca.* 1.8 V vs Fc. The high positive potential is consistent with oxidation of a cation. When the temperature was raised, this new peak gradually diminished in height, several new and ill-defined signals appeared, and the signal due to **2** became 4–6 times as intense as before the temperature increase. This suggests that the wave at 1.8 V vs Fc arises from a precursor to **2**, possibly **3** or **4**. During a two-scan CV experiment, the signal quality was too poor (especially during the second scan) to tell whether the curve-crossing/surface effects had changed.

Discussion of the Source of the Curve-Crossing Phenomenon. The cyclic voltammetry and constant-current coulometry analyses at the Au disk electrode show that **1** undergoes an irreversible one-electron oxidation at E_p = 0.13 V vs Fc. The follow-up reaction of $\mathbf{1}^{\bullet+}$ leads to the essentially quantitative formation of $Cp^*Ru(PPh_3)(NCMe)_2^+$. The coulometry data require that all hydride ligands form only H_2 (by charge balance).

The results from the CV experiments performed at the Pt electrode support the view that H_2 is liberated as a consequence of the oxidation. The position of the new oxidation wave that appeared during the second scan (Figure 3) coincides with the position of the new wave that appeared during the *first* scan in the presence of H_2 and with the (albeit irreproducible) position of the peak seen for electrolyte saturated with 3% H_2/97% N_2, and it is likely that the effects have a common origin in the H^+/H_2 redox process.

During the first anodic scan of the double-scan experiment, there is no H_2 present, and so only the normal oxidation wave due to **1** is seen. During the follow-up reactions of **1**, H_2 is liberated from reaction intermediates (slowly from **3**, and rapidly from **4**, according to the previous discussion) along with the reaction pathway from $\mathbf{1}^{\bullet+}$. Much of the H_2 thus generated is likely to diffuse away from the electrode, but some is adsorbed and undergoes oxidation to generate H^+. A highly efficient H^+ production this way normally should lead to a multielectron process. However, if one assumes that only part of the H_2 is oxidized to H^+ and that this H^+ protonates unoxidized **1** in solution (eq 4), **3** is still generated but without the involvement of direct electrooxidation of **1**. The adsorption of H_2 also readily explains the absence of the substrate oxidation wave during the second voltammetry scan. The oxidation of H_2 (peak f in Figure 3) takes place first, generating H^+, the presence of which leads to the protonation of **1** near the electrode. The substrate therefore is "removed" from the vicinity of the electrode before it has the chance to be electrooxidized. The amount of H_2 present must determine the extent of H^+ production, and therefore the relative intensity of the oxidation wave for **1** in Figure 4A–C decreases with increasing H_2 concentration. A one-electron process still is the result. The fact that a one-electron process was seen indeed is an indication that the H_2 adsorption/oxidation was not highly efficient.

As stated earlier, the "yield" of **2** is dependent on sweep rate. If at least part of the H_2 is generated at a relatively slow rate on the CV time scale, the curve crossing can be readily explained. This is so because, during the cathodic voltammetry scan, H_2 is still produced (by elimination from **3**) at a steady rate, *even when the electrode potential is on the cathodic side of the oxidation potential for* **1**. This means that the oxidizable species H_2 is generated chemically in the vicinity of the electrode during the reverse scan. This will give rise to an extra *anodic* current contribution during the cathodic scan—and the curve crossing results. (If the production of H_2 is extremely fast on the experimental time scale, then a multielectron process should ensue and no other unusual voltammetric behavior is to be expected.) The curve crossing therefore is an indication that the H_2 liberation takes place at a rate that is *moderately slow* on the voltammetric time scale. This is of course consistent with the earlier discussion of the sweep-rate-dependent "yield" of **2**.

Conclusions

The chemical and electrochemical oxidation of **1** leads to the generation of a Brønsted-acidic cation radical $\mathbf{1}^{\bullet+}$, which may actually be a dihydrogen complex. The cation radical reacts by transfer of a proton to a suitable base. The first stable products that are formed when no external base is added are $Cp^*Ru(PPh_3)(NCMe)H_2^+$ and $Cp^*Ru(PPh_3)H_4^+$, which in secondary reactions release H_2(g) at different rates. The production of H_2 leads to rather unusual voltammetric behavior at the Pt electrode. The cyclic voltammetry curve crossing indicates that part of the H_2 generation takes place at a rate that is moderately slow on the voltammetric time scale.

Following the findings reported here, one may expect complications arising from the liberation of H_2 to occur for other metal hydride oxidations. We note that a curve crossing in an unusual two-cycle voltammogram was reported, but not fully explained, for the oxidation of *fac*-$Ir(PMe_2Ph)_3H_3$ at the Pt electrode.[3a] A somewhat less striking curve-crossing phenomenon was seen during the oxidation of $ReH_7(PPh_3)_2$, and it was indicated that it could be caused by the liberation of H_2(g).[3b]

The results presented here should help understand the behavior of electrochemical studies of metal hydrides at the Pt electrode. It is recommended that other electrode materials be used (Au or glassy carbon) if the complications arising from H_2 are to be avoided. However, with the insight provided here in mind, useful and complementary information can also be obtained with the Pt electrode.

Experimental Section

General Procedures. All manipulations involving organometallic compounds were carried out with the use of vacuum line, Schlenk, syringe, or drybox techniques. Acetonitrile was distilled from P_2O_5, and

(15) Kolthoff, I. M.; Chantooni, M. K., Jr. *J. Phys. Chem.* **1972**, *76*, 2024.
(16) Compound **1** is detectably (76%) decomposed by CH_2Cl_2 in 2.5 h at 21 °C, which necessitates this reduced temperature.

acetonitrile-d_3, dichloromethane, and dichloromethane-d_2 were distilled from CaH_2. Ether and THF were distilled from sodium benzophenone ketyl. THF-d_8 was distilled from potassium metal. All deuterated solvents, after drying over the appropriate drying agent, were vacuum-transferred, degassed, and stored in the drybox.

^1H NMR spectra were recorded on Nicolet 360 and Bruker AM 500 instruments on 0.1 M solutions. Chemical shifts are reported in ppm relative to tetramethylsilane, with the residual solvent proton resonance as internal standards (δ 1.93 for acetonitrile-d_3, δ 3.58 for THF-d_8, δ 5.32 for dichloromethane-d_2). ^{31}P NMR chemical shifts were referenced to external 85% H_3PO_4 at 0.00 ppm with shifts downfield of the reference considered positive. ^1H NMR T_1 measurements were carried out at 500 MHz by the inversion recovery method using a standard 180°–τ–90° pulse sequence. Values of $T_{1(min)}$ and the temperature at which it occurred are accurate to ±5% and ±2 °C, respectively.

Infrared spectra were measured on a Nicolet 510P-FT infrared spectrophotometer. The electrochemical instrumentation, cells, data-handling procedures, and electrodes have been previously described.[17] When used as the solvent for electrochemical measurements, acetonitrile containing 0.1 M $Bu_4N^+PF_6^-$ or dichloromethane containing 0.2 M $Bu_4N^+PF_6^-$ was passed through a column of active, neutral alumina before use to remove water and protic impurities. The electrolyte was freed of air by purging with purified argon, and all electrochemical experiments were conducted under a blanket of solvent-saturated argon at 20 °C unless otherwise noted.

$Cp^*Ru(PPh_3)(H)_3$ was synthesized according to the published procedure.[18a] The required Ru(III) precursor was prepared from $(Cp^*RuCl_2)_n$[18b] and PPh_3 in ethanol. $Cp_2Fe^+PF_6^-$ was prepared according to the literature procedure.[18c] $HBF_4{\cdot}Et_2O$ (Aldrich, 85%) was used as received. Et_3N (Aldrich) was distilled before use and stored over 4-Å molecular sieves in a flask that was protected from light. Quinuclidine (Aldrich) was distilled before use. 2,6-Di-*tert*-butyl-4-methylpyridine (Aldrich) was used as received.

$Cp^*Ru(PPh_3)H_4^+BF_4^-$. In the drybox, an NMR tube equipped with a screw cap and septum was loaded with **1** (47 mg, 0.093 mmol) and dichloromethane-d_2 (*ca.* 1 mL). The capped NMR tube was immediately removed from the drybox and put in a Dewar flask precooled at –80 °C with an ethyl acetate–dry ice slurry. $HBF_4{\cdot}Et_2O$ (18 μL, 0.102 mmol) was added to the tube with a gastight microsyringe. The tube was shaken once, and the NMR spectra were recorded immediately. ^1H NMR (–65 °C, dichloromethane-d_2): δ –7.4 (br s, 4H), 1.7 (s, 15H), 7.3–7.5 (m, 15H). ^{31}P NMR (–65 °C, dichloromethane-d_2): δ 51.4 (s).

Synthesis of $Cp^*Ru(PPh_3)(NCMe)_2^+BF_4^-$ by Acidolysis of 1. In the drybox, a 100-mL Schlenk flask with a septum was charged with **1** (135 mg, 0.269 mmol) and acetonitrile (27 mL). The flask was taken out of the drybox, and $HBF_4{\cdot}Et_2O$ (50 μL, 0.285 mmol) was added using a gastight microsyringe. Gas evolution was observed. After $^1/_2$ h, the brown, almost clear, suspension turned lighter brown and cleared considerably. The mixture was stirred further for $1^1/_2$ h at 25 °C. The solvent was removed by vacuum transfer, and the residue was dried for 2 h under vacuum. Yield: 140 mg (78%) of a greenish-yellow microcrystalline powder. The exact amount of $HBF_4{\cdot}Et_2O$ used in this reaction is important, since greater excess leads to the formation of a side product. IR (Nujol): 1150 (shoulder, s), 1093 (vs), 1057 (vs), 1028 (vs), 999 (sharp shoulder, s), 976 (shoulder, s), 889 (w), 841 (m), 750 (m), 699 (vs), 526 (vs), 515 (s), 501 cm^{-1} (m). ^1H NMR (acetonitrile-d_3): δ 1.42 (d, J = 1.7 Hz, 15H), 1.99 (br s, 6H), 7.41–7.49 (m, 15H). $^{31}P\{^1H\}$ NMR (acetonitrile-d_3): δ 48.7 (s).

Synthesis of $Cp^*Ru(PPh_3)(NCMe)_2^+PF_6^-$ by Oxidation of 1. In the drybox, a 100-mL Schlenk flask was charged with **1** (52 mg, 0.104 mmol) and acetonitrile (9 mL). To the resulting brown suspension was added dropwise $Cp_2Fe^+PF_6^-$ (33 mg, 0.10 mmol) in acetonitrile (2 mL). Gas evolution was observed. The mixture was stirred for 2 h. The solvent was removed in vacuo, and the residue was dried for 2 h under vacuum. $^{31}P\{^1H\}$ NMR (acetonitrile-d_3): δ 49.1 (s), –143 (heptet, J = 707 Hz, PF_6^-). ^1H NMR: as described above.

An experiment in which 2 equiv of $Cp_2Fe^+PF_6^-$ was used had no effect on the reaction except for the incomplete consumption of $Cp_2Fe^+PF_6^-$, as evidenced by the lack of a Cp_2Fe ^1H NMR signal due to rapid electron self-exchange with remaining Cp_2Fe^+.

Preparation of $Cp^*Ru(PPh_3)(NCMe)_2^+BF_4^-$ by Electrochemical Oxidation of 1. The preparative electrolysis was carried out in a H-shaped cell, the compartments of which were separated by a fritted-glass junction. A Pt gauze working electrode was used. Each compartment was filled with 20 mL of acetonitrile/0.05 M $Me_4N^+BF_4^-$, and the electrolyte was freed of air by purging with argon. The anodic compartment was loaded with **1** (20 mg, 0.040 mmol). The oxidation was performed at a constant current of 10 mA while the progress of the electrolysis was monitored at an Au electrode by cyclic voltammetry. The signal due to the oxidation of **1** was completely gone after the passage of 1.02 faradays/mol of charge. The anolyte was transferred to a round-bottom flask, and the solvent was removed by vacuum transfer. The residue was extracted with dichloromethane (2 × 5 mL), the combined extracts were filtered (fine fritted glass, Celite), and the filtrate was evaporated to dryness to yield a light greenish-orange solid (18 mg, 67%) that was found to be *ca.* 90% pure **2**(BF_4^-) by ^1H NMR spectroscopy.

Oxidation of $Cp^*Ru(PPh_3)(H)_3$ with $Cp_2Fe^+PF_6^-$ in the Presence of 2,6-Di-*tert*-butyl-4-methylpyridine. In the drybox, a 100-mL Schlenk flask was charged with **1** (70 mg, 0.139 mmol) and acetonitrile (10 mL). To the resulting suspension was added the amine (800 mg, 4.41 mmol). A solution of $Cp_2Fe^+PF_6^-$ (35 mg, 0.105 mmol) in acetonitrile (1 mL) was added. No gas evolution was observed. The mixture was stirred for 2 h, and the solution was then concentrated to *ca.* 30% of the original volume by vacuum transfer. An aliquot of the reaction mixture was assayed by $^{31}P\{^1H\}$ NMR to reveal the presence of equimolar amounts of **1** and **2**. The aliquot was returned to the Schlenk flask. Another 35 mg (0.105 mmol) of $Cp_2Fe^+PF_6^-$ in acetonitrile (2 mL) was added to the mixture. Gas evolution was seen. Stirring was continued for 2 h. The $^{31}P\{^1H\}$ NMR analysis now indicated full conversion of **1** to **2**.

Detection of $Cp^*Ru(PPh_3)(NCMe)H_2^+$ by NMR Spectroscopy. To a solution of **1** (42 mg, 0.084 mmol) in dichloromethane-d_2 (1 mL) was added acetonitrile-d_3 (0.1 mL, 1.9 mmol). The mixture was cooled to –80 °C in an NMR tube, and $HBF_4{\cdot}Et_2O$ (*ca.* 1 μL, 0.06 mmol) was added. NMR spectra recorded immediately at –65 °C in a precooled probe revealed (by ^{31}P NMR) unreacted **1** (*ca.* 5%), $Cp^*Ru(PPh_3)H_4^+$ (75%), $Cp^*Ru(PPh_3)(NCMe)_2^+$ (15%), and *ca.* 3% each of two products (δ 62.5 and 60.8), one of whose peaks is assigned to $Cp^*Ru(PPh_3)(NCMe)H_2^+$. The ^1H NMR spectrum of the same solution at –65 °C showed a hydride doublet (δ –6, J = 19 Hz) assigned to $Cp^*Ru(PPh_3)(NCMe)H_2^+$. Hydride signals due to **1** (13%) and $Cp^*Ru(PPh_3)H_4^+$ (78%) were also seen. The low concentration of $Cp^*Ru(PPh_3)(NCMe)H_2^+$ relative to $Cp^*Ru(PPh_3)H_4^+$ and $Cp^*Ru(PPh_3)(NCMe)_2^+$ suggests that $Cp^*Ru(PPh_3)(NCMe)H_2^+$ is consumed by acetonitrile slightly faster than $Cp^*Ru(PPh_3)H_4^+$.

Deprotonation of $Cp^*Ru(PPh_3)H_4^+BF_4^-$. In the drybox, an NMR tube equipped with a screw cap and septum was charged with **1** (21 mg, 0.042 mmol) and dichloromethane-d_2 (0.7 mL). The tube was placed in a Dewar flask cooled at –80 °C, $HBF_4{\cdot}Et_2O$ (*ca.* 9 μL, 0.050 mmol) was added to the tube with a gastight syringe, and the tube was shaken once. ^1H and ^{31}P NMR spectra were recorded at –65 °C to reveal the presence of $Cp^*Ru(PPh_3)H_4^+$. The NMR tube was taken back to the Dewar flask, and Et_3N (*ca.* 30 μL, 0.21 mmol) was added. The ^{31}P NMR spectrum revealed clean and quantitative conversion of $Cp^*Ru(PPh_3)H_4^+$ into **1**. *Note*: The hydride-proton-coupled ^{31}P NMR spectrum of **1** usually failed to show resolved coupling. However, in this deprotonation experiment, the coupled spectrum revealed a well-resolved quartet with J = 15 Hz.

Acknowledgment. We gratefully acknowledge support from Statoil under the VISTA program, administered by the Norwegian Academy of Science and Letters, from the Norwegian Council for Science and the Humanities (NAVF), from the U.S. National Science Foundation, and from NATO under Grant No. CRG 910473.

(17) Tilset, M. In *Energetics of Organometallic Species*; Simões, J. A. M., Ed.; Kluwer Academic: Dordrecht, The Netherlands, 1992; p 109.

(18) (a) Suzuki, H.; Lee, D. H.; Oshima, N.; Moro-oka, Y. *Organometallics* **1987**, *6*, 1569. (b) Oshima, N.; Suzuki, H.; Moro-oka, Y. *Chem. Lett.* **1984**, 1161. (c) Lyatifov, P. R.; Solodovnikov, S. P.; Babin, V. N.; Materikova, R. B. *Z. Naturforsch., B* **1979**, *34B*, 863.